*Published online 6 December 2007*

*Nucleic Acids Research, 2008, Vol. 36, No. 2* ***e10***
*doi:10.1093/nar/gkm1081*

# Use of a multi-thermal washer for DNA microarrays simplifies probe design and gives robust genotyping assays

**Jesper Petersen[1], Lena Poulsen[2], Sarunas Petronis[3], Henrik Birgens[1] and Martin Dufva[2,*]**

[1]Department of Haematology, Herlev Hospital, University of Copenhagen, Herlev Ringvej 75, DK-2730 Herlev, Denmark, [2]Microarray Group, Department of Micro and Nanotechnology, Technical University of Denmark, Oersteds Plads, Bld. 345 East, DK-2800 Kongens Lyngby, Denmark and [3]Department of Applied Physics, Fysikgården 4, Chalmers University of Technology, SE-412 96 Göteborg, Sweden

Received October 4, 2007; Revised and Accepted November 16, 2007

## ABSTRACT

**DNA microarrays are generally operated at a single condition, which severely limits the freedom of designing probes for allele-specific hybridization assays. Here, we demonstrate a fluidic device for multi-stringency posthybridization washing of microarrays on microscope slides. This device is called a multi-thermal array washer (MTAW), and it has eight individually controlled heating zones, each of which corresponds to the location of a subarray on a slide. Allele-specific oligonucleotide probes for nine mutations in the beta-globin gene were spotted in eight identical subarrays at positions corresponding to the temperature zones of the MTAW. After hybridization with amplified patient material, the slides were mounted in the MTAW, and each subarray was exposed to different temperatures ranging from 22 to 40°C. When processed in the MTAW, probes selected without considering melting temperature resulted in improved genotyping compared with probes selected according to theoretical melting temperature and run under one condition. In conclusion, the MTAW is a versatile tool that can facilitate screening of a large number of probes for genotyping assays and can also enhance the performance of diagnostic arrays.**

## INTRODUCTION

Allele-specific hybridization (ASH) to DNA microarrays is a powerful method of high-throughput genotyping that is widely used by Affymetrix, as well as many other companies, for analysis of single nucleotide polymorphisms (SNPs) (1,2). Nonetheless, genotyping by ASH entails three notable difficulties. First, the performance of ASH probes depends on both the type of mutation in question (substitution or insertion/deletion) and the nucleotide sequence surrounding the mutation (2,3). Second, at present it is difficult to predict probe characteristics on the basis of thermodynamic models because surface effects are normally not accounted for (4,5). An exception to this is the Hyther server (6), which uses data obtained on a single substrate to calculate thermodynamic parameters, and hence it is not directly applicable to many of the commonly used substrates. Third, as microarray analysis generally is performed using a single working condition (i.e. one hybridization or stringency washing temperature), all probes must have the same thermodynamic behavior in order to operate optimally in the array. This poses a problem, because AT-rich probes must be significantly longer than GC-rich probes to achieve the same melting temperature ($T_m$), and thus they are usually less efficient at discriminating mismatch hybrids. For these reasons, the development of DNA microarrays for genotyping of small genetic variations is an extensive trial and error process.

In contrast, in methods that do not depend on a common working condition for the immobilized probes, assignment of genotypes is achieved by precise determination of melting points (7–11). Temporal gradients require specialized equipment for real-time observation of hybridization or dissociation reactions. However, many such instruments have a relatively low sample throughput, and they are limited with regard to the size of the microarray that can be investigated. An exception to this is the use of temporal gradients in combination with a scanning microscope to allow analysis of larger arrays (12). Another way of creating different conditions over an array is to use a device with spatial gradients (13,14), in which microarrays are located in different thermal zones to create optimal conditions for ASH. The shortcomings

*To whom correspondence should be addressed. Tel: +45 4525 6324; Fax: +45 4588 7762; Email: mdu@mic.dtu.dk

The authors wish it to be known that, in their opinion, the first two authors should be regarded as joint First Authors.

of such devices include the following: incompatibility with microarray scanners (13), small heating zones (13,14), limited temperature control (14), complex fabrication (13) and demanding alignment of DNA microarrays (13,14).

Here, we describe the design and manufacture of a microfluidic device containing eight relatively large, individually controlled heating zones for multi-stringency posthybridization washing of microarrays printed on glass microscope slides. The usability of this multi-thermal array washer (MTAW) was demonstrated by genotyping a small cohort of patients for mutations in the beta-globin gene.

## MATERIALS AND METHODS

### Design and fabrication of the MTAW

The washer consisted of (i) a solid support containing heaters and temperature probes, (ii) an elastic layer containing microfluidic chambers and channels, and an alignment groove for a slide and (iii) a pressure lid (Figure 1B and C). The heater support was fabricated directly in a printed circuit board (PCB) by photolithographic patterning and wet-copper etching. The resistive heaters were made out of narrow zigzag copper wires attached to wide leads for electrical connection. To prevent the heaters from chemical and electrical interaction with the washing fluids, the PCB surface was subsequently spray-coated with a conformal layer of silicone (RS Components Ltd, Northants, UK). Holes for the temperature probes (TS67-170 microthermistors, Oven Industries Inc., Mechanicsburg, PA, USA) were drilled in the support at the periphery of each heater. The thermistors were fixed in place with semi-flexible UV-curable glue (Dymax 952/-T, DYMAX Corp., Torrington, CT, USA).

The elastic layer of the polydimethylsiloxane (PDMS) fluidic structure was molded directly on top of the support, so that each chamber (temperature zone) was located straight above a heater. The polymethylmethacrylate (PMMA) master structures were micromachined on a laser ablation system (Synrad Inc., Mukilteo, WA, USA) controlled by CAD software (winMark Pro, Synrad). The PDMS prepolymer and catalyst (Sylgard 184, Dow Corning, Germany) were mixed and degassed under vacuum for 20 min, after which a PMMA frame was mounted on the PCB and the PDMS prepolymer mixture

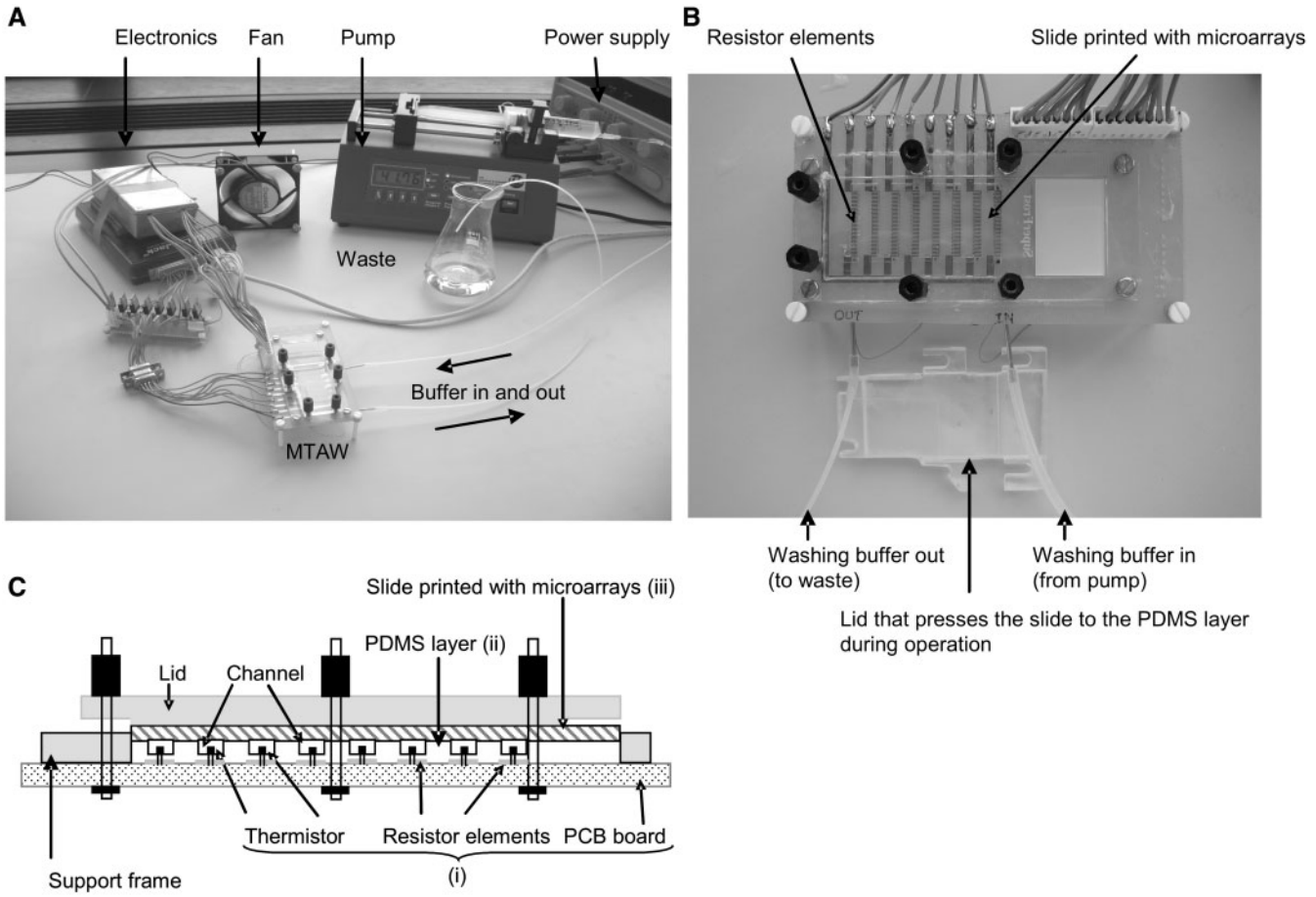


**Figure 1.** The multi-thermal array washer (MTAW). (A) Photograph showing the experimental setup used to wash slides in the device. (B) Photograph of the assembled MTAW. (C) Schematic drawing of an assembled system viewed from the side. The main parts of the device are shown: (i) the PCB board, microheaters, and thermistors, including a slide holder attached to a layer of polydimethylsiloxane (PDMS); (ii) the PDMS layer, which defines the fluidic channels and chambers above the heaters; (iii) the microscope slide printed with identical subarrays that face towards corresponding chambers after the device is sealed.

was poured inside the frame. The PMMA master defining the microfluidic structures was immersed in the PDMS prepolymer, and the structure was subsequently covered with a PMMA plate with the same dimensions as a microscope slide. The PDMS was cured for 3 h at 80°C, after which the PMMA plate and insert were removed, which resulted in an open fluidic system and an alignment groove for the microscope slide.

### Temperature control

In our experiments, the MTAW was controlled by use of a LabJack U12 data acquisition card (LabJack Corporation, Lakewood, CO, USA) and a computer code based on LabView v8.0 software (National Instruments, Austin, TX, USA). For temperature measurements, the resistance reading for each thermistor mounted in the washing chambers was recorded as the voltage drop across the thermistor when a constant current of 50 μA was applied using home-built electronic circuits (Figure 1A). The resistance was then converted into temperature by a LabView code using second-order approximation of the Steinhart-Hart equation and fitting parameters determined by experimental calibration.

The heaters (resistor elements; shown in Figure 1B and C) were controlled by pulse length modulation of the applied electrical power. The pulse-length-modulating algorithm was based on a modified proportional controller, and additional protection against temperature overshoot was achieved by power cutoff if the heating rate exceeded a certain value when close to the set-point temperature. The pulse length was controlled by the digital outputs of the LabJack card, which were connected to the home-built electronic circuit and thereby supplied power to the heaters (Figure 1A).

The flow was directed from the low to the higher temperature zones on the microarray slide, so that the fluid had been preheated in previous chambers upon reaching the subsequent warmer chamber. This was done to enable uniform temperature distribution along the chambers.

The thermistors were calibrated every second day by placing the MTAW in an incubator at 60°C and subsequently at 20°C. During use, an 80 mm 12 V cooling fan was placed at a distance of ~15 cm from the device to reduce any heating caused by thermal conductivity on the side of the glass slide opposite the printed microarrays (Figure 1A).

### Preparation of microarrays

Allele-specific DNA probes were designed for genotyping small genetic variations in the human beta-globin gene (*HBB*). The probes had the variant base/bases positioned as close to the center of the probe as possible, and they contained a poly(T)–poly(C) tag (TC tag) in the 5′ end (15). The TC tag increases hybridization signal by unknown mechanisms that may include increasing the probe immobilization efficency during UV cross-linking and increasing hybridization efficiency by functioning as a spacer. A $T_m$-matched probe set was designed based on the following inclusion criteria: the probes were to be at least 15 nucleotides (nts) in length (16) in order to yield a sufficiently strong hybridization signal, and the range of $T_m$ values was to be as narrow as possible over the entire set (Table 1) (17).

Microarray substrates were prepared by grafting agarose film containing reactive aldehyde groups onto unmodified glass microscope slides as previously described (15,18). DNA probes (Table 1) were diluted in MilliQ water to a final concentration of 100 μM and then contact-printed in microarrays on slides coated with agarose film as mentioned (15,18). The probes were immobilized by UV irradiation at 254 nm for 4 min. Thereafter, the slides were washed for 10 min in 0.1 × SSC supplemented with 0.5% SDS and then for 10 min in 0.1 × SSC to remove unbound probes. Finally, the slides were dried by centrifugation.

### DNA samples and target preparation

The DNA samples used in this study originated from individuals that were heterozygous ($n = 26$) or homozygous ($n = 2$) for a mutation in the *HBB* gene and from control subjects ($n = 4$) with no *HBB* mutations. The original diagnosis was made by measuring the level of $HbA_2$ by high-performance liquid chromatography (HPLC), and genotyping was accomplished by automated DNA sequencing.

A 300 bp portion of the *HBB* gene, containing exon I and the first part of intron I, was amplified by PCR using the primer pair BCF and T7-BCR (Table 1). PCR amplification of DNA samples was performed in a total volume of 80 μl containing 1 μM of each primer BCF and T7-BCR, 200 μM of each dNTP, 0.1 U/μl TEMPase Hot Start DNA polymerase (Ampliqon, Bie & Berntsen A/S, Rødovre, Denmark) and 1 × TEMPase Buffer II provided with the enzyme. The reverse primer T7-BCR contained a T7 promoter sequence in the 5′ end and thereby served as DNA template for subsequent T7 RNA polymerase amplification. The PCR cycling conditions were 15 min at 95°C followed by 35 amplification cycles at 95°C for 30 s, 60°C for 45 s, 72°C for 1 min, and a final extension at 72°C for 10 min. PCR products were confirmed on an Agilent Bioanalyzer 2100 (Agilent Technologies, Palo Alto, CA, USA) using a DNA 500 LabChip kit (Agilent Technologies). The PCR products were used directly (without purification steps) as a template for the T7 *in vitro* transcription (IVT).

Single-stranded RNA target was produced by T7 IVT in an 80 μl reaction mixture containing 8 μl of template DNA, 500 μM of each NTP, 12.5 μM (2.5%) Biotin-11-UTP (PerkinElmer Life and Analytical Sciences, Boston, MA, USA), 1 U/μl T7 RNA Polymerase-Plus™ (Ambion, Huntingdon, Cambridgeshire, UK) and 1 × transcription buffer provided with the enzyme. The reaction was performed at 37°C for 2 h, which resulted in ~200 ng/μl amplified RNA. Since each slide was hybridized with 80 μl of RNA in a total hybridization volume of 160 μl, the concentration of the 300-nt-long RNA fragment during hybridization was estimated to be 1 μM.

### Hybridization and multi-thermal washing

RNA target was diluted 1 : 1 in hybridization buffer to a final concentration of 5 × SSC and 0.5% SDS.

**Table 1.** DNA oligonucleotide probes and primer

| Probe name | Sequence | $T_m$ (°C)[a] |
|---|---|---|
| Re-designed shorter probes | | |
| CD24 mt (13) | TTTTTTTTTTCCCCCCCCCCGTTGGAGGTGAGG | 39.8 |
| CD24 wt (13) | TTTTTTTTTTCCCCCCCCCCGTTGGTGGTGAGG | 40.6 |
| CD27-28 mt (13) | TTTTTTTTTTCCCCCCCCCCGAGGCCCCTGGGC | 52.2 |
| CD27-28 wt (13) | TTTTTTTTTTCCCCCCCCCCGAGGCCCTGGGCA | 50.5 |
| CD27-28 mt (12) | TTTTTTTTTTCCCCCCCCCCGAGGCCCCTGGG | 47.2 |
| CD27-28 wt (12) | TTTTTTTTTTCCCCCCCCCCGAGGCCCTGGGC | 48.2 |
| $T_m$-matched probe-set | | |
| CD5 mt | TTTTTTTTTTCCCCCCCCCCCGCACCTGACTCGAGGAGAAGT | 54.9 |
| CD5 wt | TTTTTTTTTTCCCCCCCCCCCGCACCTGACTCCTGAGGAGAA | 54.7 |
| CD8 mt | TTTTTTTTTTCCCCCCCCCCCCCTGAGGAGGTCTGCCG | 54.0 |
| CD8 wt | TTTTTTTTTTCCCCCCCCCCCCCTGAGGAGAAGTCTGCCG | 53.7 |
| CD8-9 mt | TTTTTTTTTTCCCCCCCCCCCGAGGAGAAGGTCTGCCGTTAC | 53.5 |
| CD8-9 wt | TTTTTTTTTTCCCCCCCCCCCGAGGAGAAGTCTGCCGTTACTG | 53.4 |
| CD15 mt | TTTTTTTTTTCCCCCCCCCCCACTGCCCTGTAGGGCAAGGT | 57.4 |
| CD15 wt | TTTTTTTTTTCCCCCCCCCCCTGCCCTGTGGGGCAAGG | 57.6 |
| CD17 mt | TTTTTTTTTTCCCCCCCCCCCCCCTGTGGGGCTAGGTGA | 55.4 |
| CD17 wt | TTTTTTTTTTCCCCCCCCCCCCCCTGTGGGGCAAGGTG | 55.4 |
| CD24 mt | TTTTTTTTTTCCCCCCCCCCCAAGTTGGAGGTGAGGCCCT | 54.8 |
| CD24 wt | TTTTTTTTTTCCCCCCCCCCCGAAGTTGGTGGTGAGGCCC | 54.9 |
| CD27-28 mt | TTTTTTTTTTCCCCCCCCCCCGTGAGGCCCCTGGGC | 55.7 |
| CD27-28 wt | TTTTTTTTTTCCCCCCCCCCCGTGAGGCCCTGGGCAG | 55.3 |
| IVS I + 5 mt | TTTTTTTTTTCCCCCCCCCCGGCAGGTTGCTATCAAGGTTACA | 53.5 |
| IVS I + 5 wt | TTTTTTTTTTCCCCCCCCCCGGCAGGTTGGTATCAAGGTTACA | 53.3 |
| IVS I + 6 mt | TTTTTTTTTTCCCCCCCCCCGGCAGGTTGGCATCAAGG | 53.1 |
| IVS I + 6 wt | TTTTTTTTTTCCCCCCCCCCGGCAGGTTGGTATCAAGGTTACA | 53.3 |
| PCR primers | | |
| BCF | AGCAGGGAGGGCAGGAGCCA | |
| T7-BCR | GAAATTAATACGACTCACTATAGGGAGAAGAGTCAGTGCCTATCAGAAACCC | |

[a]The melting temperatures were estimated by using the freely available oligonucleotide analyzer software provided by integrated DNA technologies at http://www.idtdna.com/analyzer/Applications/OligoAnalyzer/. Settings were chosen to be at an oligonucleotide concentration of 0.1 μM and with a monovalent salt concentration of 36.7 mM.

The mixture was heat denatured (1 min at 95°C) and immediately placed over the entire surface of an agarose-coated slide, using another microscope slide as a cover during hybridization (2 h at 37°C) in a humid chamber. After hybridization, the slide was mounted in the MTAW and washed with 0.2 × SSC + 0.1% SDS for 30 min at temperatures ranging from 22 to 40°C. The syringe pump (Figure 1A) gave a flow rate of 0.2 ml/min.

### Detection and analysis

The microarrays were stained with a 1 : 500 dilution of streptavidin Cy3-conjugate (Sigma–Aldrich) in 2 × phosphate-buffered saline (PBS) (Bie & Berntsen A/S) for 30 min in a humid chamber at room temperature. To remove unbound fluorescent molecules, the slides were subsequently washed in 1 × PBS for 5 min at room temperature. The microarrays were scanned in an ArrayWoRx CCD-based scanner (Applied Precision, Issaquah, WA, USA). The scanner could not scan at the perimeter of the slide containing the last subarray (located in a temperature zone of 43°C), so that subarray was not used in the analysis. All signals were analyzed with the freeware quantification program ScanAlyze version 2.50. The normalized ratio for each probe set at each temperature was calculated as the signal from the wild-type probe divided by the sum of the signals from the wild-type and mutant probes ($S_{WT}/(S_{WT} + S_{MT})$). This means that at an appropriate stringency during the posthybridization washing step, the normalized ratio of a homozygous wild type should approach an ideal value of 1.0, which represents a much more intense signal from the wild-type probe than from the mutant probe. Likewise, the ratio of a heterozygote should, at any stringency, approach 0.5. This reflects equality in the signal intensities exhibited by the corresponding wild-type and mutant probes.

## RESULTS

### Temperature control of the MTAW

A graphic representation of the temperature in each chamber during a test run is shown in Supplementary Figure 1. It took about 2 min to create a 3°C-per-step gradient ranging from 22 to 40°C. The temperatures measured in the chambers varied by only 1–4% after the desired temperatures had been established, which indicates good control of the temperature of the chip. Furthermore, routine calibration of the thermistors in the MTAW showed maximum deviations of 0.3°C and 0.5°C from the calibration temperatures of 20°C and 60°C, respectively.

To assess the homogeneity of the temperature in each chamber, a hybridized array comprising a probe pair

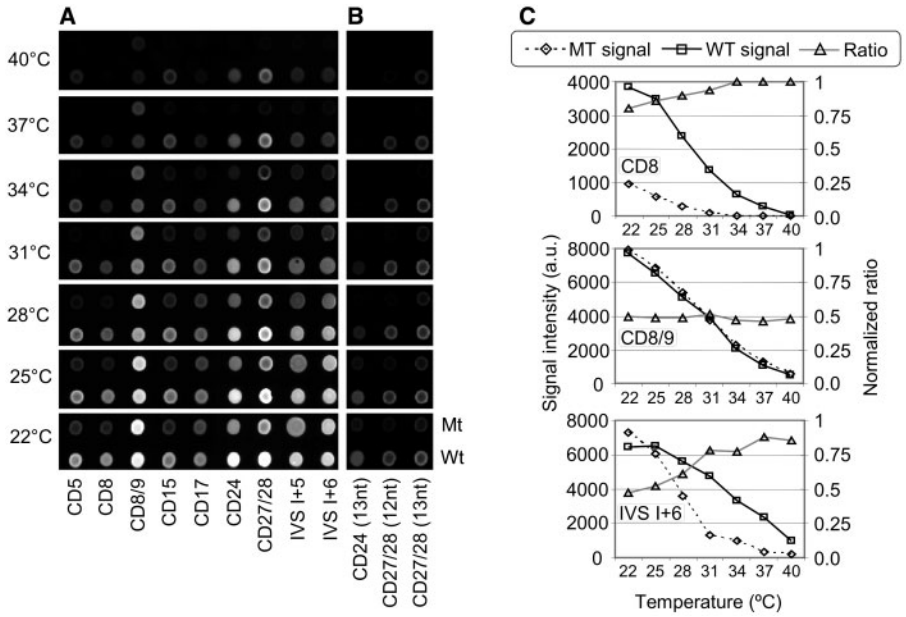


**Figure 2.** Scanning images of a processed array and corresponding melting curves. The scanning images show an array of $T_m$-matched probes (A) and three re-designed shorter probe-pairs (B) hybridized with amplified and labeled target material that was obtained from a person heterozygous for the CD8/9 + G mutation and was processed in the MTAW. The temperatures in the respective zones are denoted to the left, and the identities of the probes are indicted below the images. Wild-type probes (Wt) for the different mutations and the corresponding mutant probes (Mt) are shown at the bottom and the top of each panel, respectively. (C) Melting curves of the wild-type (square) and mutant (diamond) probes at three different mutation sites. The graphs are based on the quantified signal intensity (in arbitrary units, a.u.) of the scanning images obtained at the corresponding temperatures. The secondary Y-axes present the normalized ratio (triangle; see Materials and Methods) calculated from the signals of the wild-type and mutant probes at each of the indicated temperatures.

(CD8/9) printed along the complete length of each chamber was processed in the MTAW. The observed normalized ratios ('Materials and Methods' section) along each chamber were within the minimum/maximum values noted in our genotyping assays, which suggests that there will be no significant temperature variation within the different heating zones when the MTAW is used at the flow rate we employed in our study (0.2 ml/min). At a lower flow rate (0.05 ml/min), we found that the normalized ratios indicated a temperature gradient along each chamber, which is not desirable.

A wide temperature range of 25–60° could be generated in the device. This range was used to create two distinct melting curves, one for a perfect-match duplex and the other for a single nucleotide mismatch duplex (Supplementary Figure 2).

## Genotyping using the MTAW

The performance of the MTAW was tested using a set of $T_m$-matched probes constructed to detect mutations in the beta-globin gene. A slide was hybridized with amplified and labeled RNA derived from a person heterozygous in position CD8/9 + G and was subsequently mounted in the MTAW. The subarrays were washed for 30 min at temperatures ranging from 22 to 40°C in increments of 3°C. Figure 2A shows a scanning image of the seven subarrays. As expected, the mutant and wild-type probes for the mutation CD8/9 + G gave similar signals over the temperature range, resulting in a ratio of 0.5 at all temperatures (Figures 2 and 3). In contrast, at the mutation sites that were tested, where the subject was homozygous for the wild-type allele, we observed stronger signals from wild-type probes than from mutant probes, even at the lowest washing temperature, with the exception of mutation sites IVS-I + 5 and IVS-I + 6. The normalized ratios for homozygotes generally increased with increasing temperatures for most of the mutation sites. However, some mutations showed a loss of signal at 40°C, which led to decreased ratios (Figures 2–4).

## Comparison of different methods of genotyping using the MTAW

DNA from a total of 32 subjects was genotyped using the MTAW. Successful performance of a probe pair in genotyping of a mutation was defined as a clear perfect-match probe signal, unambiguous separation of heterozygotes from homozygotes and a normalized ratio of ~0.5 for heterozygotes. In practice we used the following criterias: wild-types should have ratios between 0.7 and 1.0, heterozygotes between 0.35 and 0.65 and mutants between 0 and 0.3. Three different methods of genotyping achieved by processing in the MTAW were compared, which used the following conditions: (i) $T_m$-matched probes at a common optimal temperature; (ii) $T_m$-matched probes at different temperatures optimal for each probe pair and (iii) probes selected for performance according to criterias given above irrespective of the calculated $T_m$.

Finding the common optimal temperature for a $T_m$-matched set [method (i) above] was simple with the

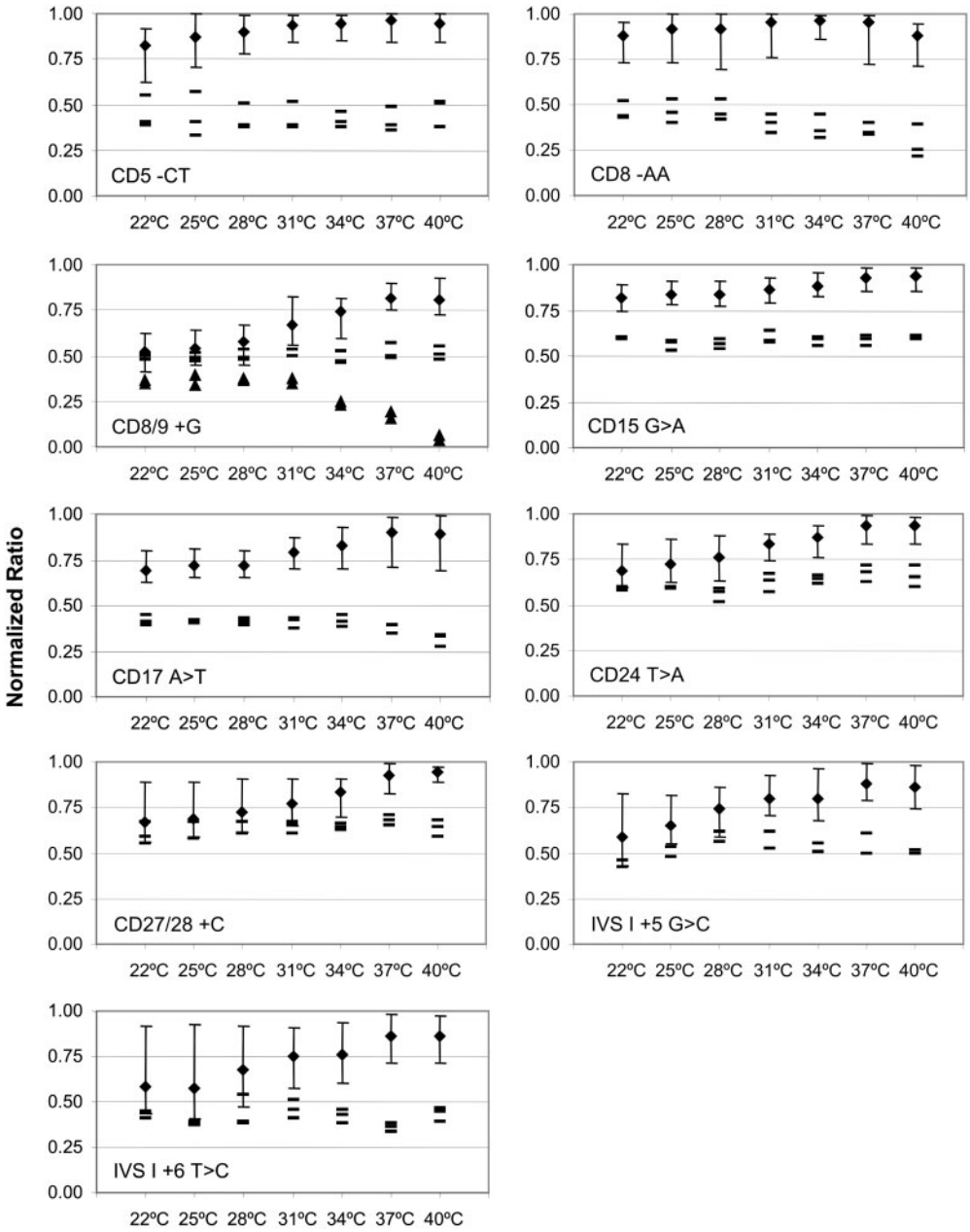


**Figure 3.** Genotyping of patient material using the MTAW and a $T_m$-matched probe set. Thirty-two different samples were individually hybridized to arrays of probes and subsequently processed in the MTAW. For each mutation site, a graph shows the normalized ratios (see Materials and Methods) at the indicated temperatures. Symbols: diamonds, the average value of all samples carrying the wild-type DNA sequence on both alleles (29 samples for all but CD8/9 and IVS I + 5, which have 27 and 30 respectively); error bars, the minimum and maximum observed ratios; dashes, the normalized ratios for heterozygous samples (three samples for each mutation site, except IVS I + 5 with only two); triangles, the normalized ratios for homozygous mutation in position CD8/9 (two samples).

MTAW, because it was a routine task to acquire data on washing carried out under different conditions. In general, the best assay performance for the respective probe pair was achieved when signals from mismatch probe hybridization were close to the background level, even if this stringency resulted in relatively weak perfect-match signals (Figures 2B and 5A, and Supplementary Figure 3). There were no misclassifications of the total of 288 genotypings at 37°C (Figures 3 and 5A). Nevertheless, when a patient was genotyped with the $T_m$-matched probe set at one level of stringency, three problems were encountered: weak signals at 37°C from CD8-AA and CD17A > T (Figure 2B and Supplementary Figure 3); large spread of heterozygotes (0.33–0.73 where 0.5 was expected), which overlapped with the lowest observed value of homozygous wild types (Figure 5A); limited separation of homozygotes and heterozygotes at all stringencies for probes specific for the CD24T>A and CD27/28 + C mutations (Figure 3 and Supplementary Figure 3).

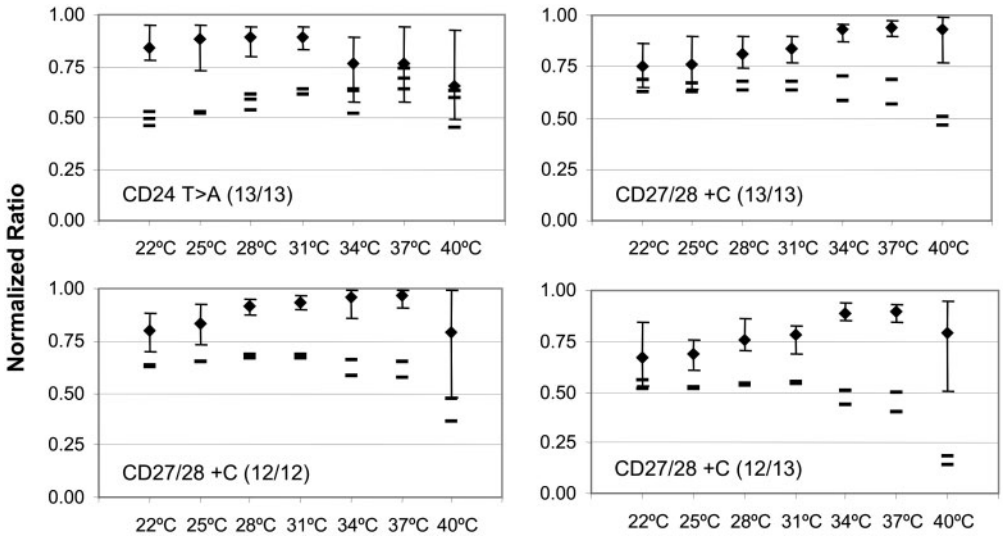


**Figure 4.** Genotyping of patient material using the MTAW and shorter redesigned probes. Thirty-two different samples were individually hybridized to arrays of shorter redesigned probes and subsequently processed in the MTAW. Calculation of normalized ratios is explained in the Materials and Methods section, and the symbols used are as described in the legend of Figure 3. The numbers within parentheses indicate the lengths of the probes (wild-type/mutant).

Utilizing the possibilities of the MTAW to apply the optimal temperature for each probe pair in the $T_m$-matched set [method (ii) above] showed that only three of the probes for the nine mutations in beta-globin functioned optimally at 37°C (Figures 3 and 5A and B). The probes for CD8-AA and CD17A>T resulted in strong signals (Figure 2 and Supplementary Figure 3) and successful separation of homozygotes and heterozygotes at 22–28°C and 31–34°C, respectively (Figure 3). The probes for IVS I + 5 G>C, IVS I + 6 T>C and CD27/28 + C separated wild types from heterozygotes better at 40°C than at 37°C, although the probe pair for CD24T>A still gave poor separation of homozygotes and heterozygotes (Figure 3). As with probes for CD24T>A, the probe pair for CD27/28 + C resulted in relatively high ratio values for heterozygotes. According to criterias given earlier, neither mutation CD24T>A nor CD27/28 + C could be genotyped using the $T_m$-matched probe set.

To further improve the genotyping assays, the probes for the mutations CD24T>A and CD27/28 + C were shortened to 12–13 nts [method (iii) above]. The truncated probes for genotyping of CD24T>A had a calculated $T_m$ of about 40°C, which is about 15°C lower than the calculated $T_m$ of the corresponding probes in the $T_m$-matched set. The shorter CD27/28 + C probes had a calculated $T_m$ of 47–52°C (Table 1). Short probes for mutation CD24T>A resulted in heterozygote ratios of about 0.5, strong signals, and successful separation of heterozygotes and homozygotes at 22°C (Figures 4 and 5C). Reducing the length of the probes for mutation CD27/28 + C to 12 or 13 nts gave satisfactory results at 37°C, although the signals were weak (Figures 4, 5 and Supplementary Figure 3). However, combining a 12-nt wild-type probe with a 13-nt mutant probe led to better separation of homozygotes and heterozygotes at 34°C (Figure 4, Supplementary Figure 3).

## DISCUSSION

DNA microarray-based assays are generally performed under one limiting condition, such as hybridization and/or posthybridization wash stringency. By comparison, our multi-thermal array washing device permits processing of arrays under multiple conditions. Thus, we were able to combine probes with different performance optima on the same array, which resulted in an assay with strong signals, unambiguous separation of homozygotes and heterozygotes, and simple classification of heterozygotes with a normalized ratio close to 0.5. Inasmuch as the MTAW allows processing of microarrays under different conditions and also provides flexibility of probe choice we were able to analyze the mutations CD8-AA, CD24T>A and CD27/28 + C in the same assay without extensive optimization.

Giving little consideration to the $T_m$ of the probes when designing DNA microarrays, as was done in our experiments, is a new concept for assays based on such collections of probes. The MTAW increases the flexibility of probe design, which is useful for site-specific applications. A number of assays offer only a limited degree of freedom to chose probes, and these methods include mutation analysis (as exemplified here), sequencing by hybridization (19), microRNA analysis (20,21) and the use of tiling arrays (22,23) or 'exon' arrays (24). According to Drobyshev *et al.* (25), even gene expression profiling can be enhanced by treating arrays at different stringencies to eliminate data from cross-hybridization of targets to probes. Those investigators repeatedly washed slides with increasing concentrations of formamide, and scanned the arrays in between the washings. Unfortunately, that procedure is cumbersome, and the repeated scans can result in photobleaching of the dyes, especially Cy5 (personal observation). By comparison, a slide processed in the MTAW is scanned only once.

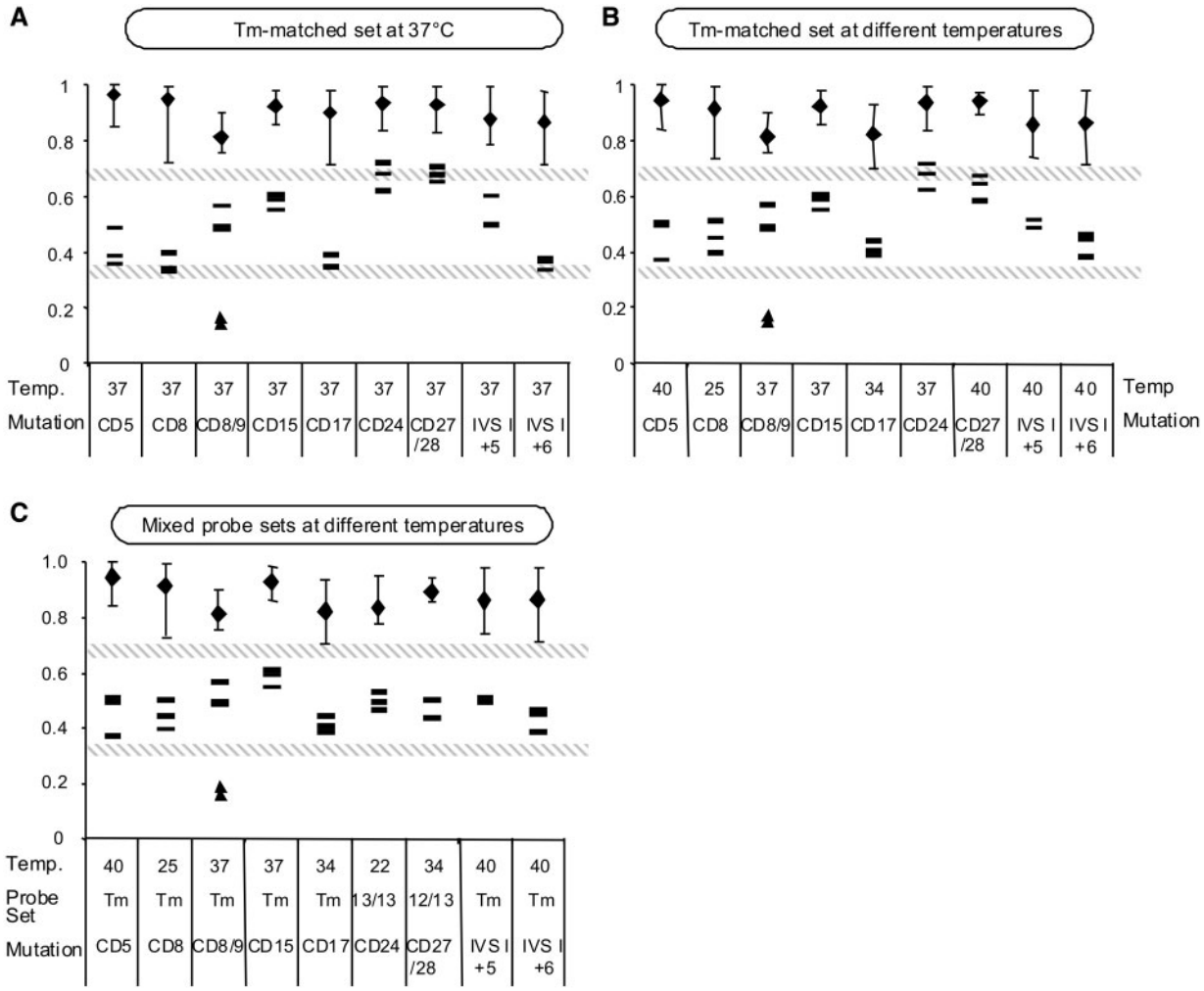


**Figure 5.** Comparison of different methods used for genotyping in the MTAW. We define successful probe pair performance when homozygotes have normalized ratio of $\geq$0.7 (wild types) or $\leq$0.3 (mutants) and heterozygotes have normalized ratio between 0.35 and 0.65. The hatched lines in the graphs indicated these boundaries. (A) $T_m$-matched probe set in which all probes were washed at the single optimal temperature of 37°C. (B) $T_m$-matched probe set in which each probe pair was washed at its optimal temperature, so that the normalized ratio of the heterozygotes was as close to 0.5 as possible. (C). A mixed set of probe pairs, all of which originated from the $T_m$-matched probe set, except those towards the CD24 and CD27/28 positions, which were substituted with shorter probes. The ratio shown for each probe pair at the temperature (°C) that was optimal for clear classification of genotypes, which is indicated by the value given above each mutation. The probe sets used are indicated as follows: $T_m$ stands for probes from the $T_m$-matched set; 13/13 denotes the 13-nt probes used for the CD24 mutation; 12/13 designates the 12-nt wild-type probes and the 13-nt mutant probes used to detect the CD27/CD28 mutation. Computation of the normalized ratio is explained in the Materials and Methods section, and the symbols used are described in the legend of Figure 3.

The MTAW can handle microarrays that are *not* enclosed in microsystems, examples of which are printed microarrays, *in situ* synthesized arrays provided by Agilent (26,27), and, after minor modifications, random bead arrays marketed by Illumina (28). To the best of our knowledge, other spatial gradient devices use arrays printed on flow cells (7,8) or on mechanically sensitive microelectronic chips (13). An obvious advantage of the MTAW is that it is fully compatible with microarray formats based on microscope slides, and thus it can be used in combination with conventional, commercially available microarray hardware such as arrayers, hybridization stations and scanners. In addition, the MTAW offers high sample throughput compared to devices that monitor dehybridization in real time, mainly because the latter usually process only a part of a slide and one slide at a time (7–9). Since dehybridization is a relatively slow operation, the time required for processing each slide can be as much as 1 h or more.

Genotyping using temporal thermal gradients is based on determination of the $T_m$ of matched and mismatched hybrids (7–9). However, recent results have suggested that an isothermal wash is preferable, because detection at different temperatures causes technical problems, such as variation in fluorescence and formation of gas bubbles (7,29,30). Furthermore, short washing cycles are the only practical solution for temporal gradients, and it is difficult to analyze the data produced by such methodology (31). The microfluidic device presented here has none of the limitations associated with temporal gradients for the

following reasons: (i) washing is done for 30 min instead of 2–3 min; (ii) scanning is carried out at one temperature and using dried slides. In other words, the MTAW combines the benefits of assaying at many different temperatures with the advantages of isothermal washing procedures (31).

With the MTAW, when the temperature giving best classification of genetic states ($T_c$) for each probe pair is known, it is possible to sort probes into the temperature zones where they perform best. Hence, instead of using identical subarrays in each chamber with a genotyping throughput of 120–1300 SNPs (depending on the method of fabrication), sorted arrays can be used to analyze up to 10 000 mutations/SNPs per slide, and each mutation is analyzed at its particular optimal temperature. Compared to other spatial gradient devices, the MTAW has larger chambers and can accommodate 5- to 75-fold larger subarrays of probes (13,14). Another important feature of our device is that it is easy to employ a computer program to select the temperatures in the heating zones, instead of positioning probes in continuous thermal gradients by use of microfluidics (14). Finally, the MTAW is completely reusable and therefore, economically more attractive than disposable microarray devices with built-in microheaters and temperature probes (13).

In our experiments, there was a large difference between the calculated $T_m$, the observed $T_m$ and the $T_c$ (Supplementary Figure 4). The observed $T_m$ represented the temperature noted at half maximum signal, and this definition was used because in most cases the plateau phases of the signals could not be discerned. Furthermore, the reaction on the chip was not at equilibrium due to constant removal of target during washing (31), and computation of the $T_m$ assumes equilibrium conditions for the probes and the targets (32). Accordingly, it is important to keep in mind that the calculated $T_m$ for hybrids in solution is only an approximation of the observed $T_m$ of immobilized probes. Thermodynamic-based calculations of the $T_m$ of duplexes in solution are fairly accurate (to within about 2°C of the observed $T_m$) (33). In contrast, calculations of solution phase $T_m$ values for probes linked to surfaces are often overestimated compared to the measured $T_m$ values (13,15,34,35). Fotin *et al.* (35) found a general decrease in $T_m$ of $20 \pm 5$°C for probes linked to polyacrylamide as compared to probes in solution. Our results showed that the observed $T_m$ was $19 \pm 5$°C lower than the calculated $T_m$, which is similar to the values reported by Fotin *et al.* Discrepancies between calculated $T_m$ and observed $T_m$ are most likely due to repulsive effects of the negative surface of the solid support and the clustering of negative charges on the DNA probes and targets in the spots (4,34,36). In the microarrays presented here, the high density of probes reduced the theoretical $T_m \sim 10^\circ$, assuming a probe density of 100 fmol/mm$^2$ (18) and using the theoretical models suggested by Vainrub *et al.* (36). Another reason for differences between calculated and observed $T_m$ is that it is difficult to estimate probe and target concentration, and the dehybridization event on a microarray usually occurs under non-equilibrium conditions.

Vainrub *et al.* (36) predicted that hybridized spots with high probe densities would have broader dissociation curves compared to such spots with low probe densities. Our data obtained using the MTAW clearly indicate broad melting curves that partly or completely cover the investigated temperature range (Figure 2B and Supplementary Figure 3). This explains why we generally noted best classification using a simple normalized ratio approach at temperatures higher than the observed $T_m$, because the ratio will be highest when one of the probe signals is close to zero. For instance, if the signal of the mismatch probes reaches zero, then the ratio will be one. However, this will be true only when the prefect-match probes generate a significant signal. In our experiments, seven probe pairs functioned well at temperatures higher than the observed $T_m$, four probe pairs performed best at observed $T_m$, and one probe pair functioned better at a temperature significantly under observed $T_m$. Thus, $T_c$ is only weakly correlated with the calculated $T_m$ or observed $T_m$ (Supplementary Figure 4). This finding corroborates results published by Kajiyama *et al.* (13), which indicate a weak correlation between the actual temperature for optimal classification and the predicted optimal temperature. It appears that factors other than $T_m$ must also be taken into consideration to successfully predict the function of immobilized probes. One such factor might be the $\Delta G$ values of the perfect-match and the mismatch hybrids, which could predict binding strengths and thus also hybridization signals (37,38). However, it appears to be difficult to foretell what levels of time and stringency will completely wash away the mismatch signal while retaining enough of the perfect-match signals. Such predictions are not within the scope of this article.

In conclusion, the MTAW appears to be useful in all cases in which probe choice is difficult because of restriction in sequences, or when prediction of probe performance is problematic. We found that the device allowed performance of a robust genotyping assay using non-$T_m$-matched probes. The MTAW also proved to be an excellent tool for optimization of microarray assays, in that it provided a simple and precise method of obtaining multi-condition data in each experiment, a feature that can lessen the need for valuable patient material. In light of our promising results obtained with the multithermal washing device, we are currently investigating the possibility of using different salinity zones instead of varied heating. The advantages of such an approach are that chambers about twice as large can be used, and the setup is simpler.

## SUPPLEMENTARY DATA

Supplementary Data are available at NAR Online

## ACKNOWLEDGEMENTS

We thank Pia Taaning for technical assistance. This work was supported by the Danish Research Council (grant #2014-00-0003, DABIC (Danska Bioinstrument centret) and a grant from the Aase and Ejnar Danielsen

Foundation, and Lena Poulsen received a grant from DTU. Funding to pay the Open Access publication charges for this article was provided by AAse and Ejnar Danielsen Foundation.

*Conflict of interest statement*. None declared.

## REFERENCES

1. Matsuzaki,H., Dong,S., Loi,H., Di,X., Liu,G., Hubbell,E., Law,J., Berntsen,T., Chadha,M. *et al.* (2004) Genotyping over 100,000 SNPs on a pair of oligonucleotide arrays. *Nat. Methods*, **1**, 109–111.
2. Syvanen,A.C. (2005) Toward genome-wide SNP genotyping. *Nat. Genet.*, **37(Suppl.)**, S5–10.
3. Vainrub,A. and Pettitt,B.M. (2004) Theoretical aspects of genomic variation screening using DNA microarrays. *Biopolymers*, **73**, 614–620.
4. Vainrub,A. and Pettitt,B.M. (2003) Surface electrostatic effects in oligonucleotide microarrays: control and optimization of binding thermodynamics. *Biopolymers*, **68**, 265–270.
5. Zhang,L., Wu,C., Carta,R. and Zhao,H. (2007) Free energy of DNA duplex formation on short oligonucleotide microarrays. *Nucleic Acids Res.*, **35**, e18.
6. Bommarito,S., Peyret,N. and SantaLucia,J. Jr (2000) Thermodynamic parameters for DNA sequences with dangling ends. *Nucleic Acids Res.*, **28**, 1929–1934.
7. Noerholm,M., Bruus,H., Jakobsen,M.H., Telleman,P. and Ramsing,N.B. (2004) Polymer microfluidic chip for online monitoring of microarray hybridizations. *Lab Chip*, **4**, 28–37.
8. Anthony,R.M., Schuitema,A.R., Chan,A.B., Boender,P.J., Klatser,P.R. and Oskam,L. (2003) Effect of secondary structure on single nucleotide polymorphism detection with a porous microarray matrix; implications for probe selection. *Biotechniques*, **34**, 1082–1086, 1088–1089.
9. Yershov,G., Barsky,V., Belgovskiy,A., Kirillov,E., Kreindlin,E., Ivanov,I., Parinov,S., Guschin,D., Drobishev,A. *et al.* (1996) DNA analysis and diagnostics on oligonucleotide microchips. *Proc. Natl Acad. Sci. USA*, **93**, 4913–4918.
10. Howell,W.M., Jobs,M., Gyllensten,U. and Brookes,A.J. (1999) Dynamic allele-specific hybridization. A new method for scoring single nucleotide polymorphisms. *Nat. Biotechnol.*, **17**, 87–88.
11. Jobs,M., Howell,W.M., Stromqvist,L., Mayr,T. and Brookes,A.J. (2003) DASH-2: flexible, low-cost, and high-throughput SNP genotyping by dynamic allele-specific hybridization on membrane arrays. *Genome Res.*, **13**, 916–924.
12. Lee,H.H., Smoot,J., McMurray,Z., Stahl,D.A. and Yager,P. (2006) Recirculating flow accelerates DNA microarray hybridization in a microfluidic device. *Lab Chip*, **6**, 1163–1170.
13. Kajiyama,T., Miyahara,Y., Kricka,L.J., Wilding,P., Graves,D.J., Surrey,S. and Fortina,P. (2003) Genotyping on a thermal gradient DNA chip. *Genome Res.*, **13**, 467–475.
14. Mao,H., Holden,M.A., You,M. and Cremer,P.S. (2002) Reusable platforms for high-throughput on-chip temperature gradient assays. *Anal. Chem.*, **74**, 5071–5075.
15. Dufva,M., Petersen,J., Stoltenborg,M., Birgens,H. and Christensen,C.B. (2006) Detection of mutations using microarrays of poly(C)10-poly(T)10 modified DNA probes immobilized on agarose films. *Anal. Biochem.*, **352**, 188–197.
16. Koehler,R.T. and Peyret,N. (2005) Thermodynamic properties of DNA sequences: characteristic values for the human genome. *Bioinformatics*, **21**, 3333–3339.
17. Petersen,J., Stangegaard,M., Birgens,H. and Dufva,M. (2007) Detection of mutations in the beta-globin gene by colorimetric staining of DNA microarrays visualized by a flatbed scanner. *Anal Biochem*, 360, 169–171.
18. Dufva,M., Petronis,S., Bjerremann Jensen,L., Krag,C. and Christensen,C. (2004) Characterization of an inexpensive, non-toxic and highly sensitive microarray substrate. *Biotechniques*, **37**, 286–296.
19. Khrapko,K.R., Lysov Yu,P., Khorlin,A.A., Ivanov,I.B., Yershov,G.M., Vasilenko,S.K., Florentiev,V.L. and Mirzabekov,A.D. (1991) A method for DNA sequencing by hybridization with oligonucleotide matrix. *DNA Seq.*, **1**, 375–388.
20. Castoldi,M., Schmidt,S., Benes,V., Noerholm,M., Kulozik,A.E., Hentze,M.W. and Muckenthaler,M.U. (2006) A sensitive array for microRNA expression profiling (miChip) based on locked nucleic acids (LNA). *RNA*, **12**, 913–920.
21. Beuvink,I., Kolb,F.A., Budach,W., Garnier,A., Lange,J., Natt,F., Dengler,U., Hall,J., Filipowicz,W. et al. (2007) A novel microarray approach reveals new tissue-specific signatures of known and predicted mammalian microRNAs. *Nucleic Acids Res*, **35**, e32.
22. Cheng,J., Kapranov,P., Drenkow,J., Dike,S., Brubaker,S., Patel,S., Long,J., Stern,D., Tammana,H. *et al.* (2005) Transcriptional maps of 10 human chromosomes at 5-nucleotide resolution. *Science*, **308**, 1149–1154.
23. Chee,M., Yang,R., Hubbell,E., Berno,A., Huang,X.C., Stern,D., Winkler,J., Lockhart,D.J., Morris,M.S. *et al.* (1996) Accessing genetic information with high-density DNA arrays. *Science*, **274**, 610–614.
24. Frey,B.J., Mohammad,N., Morris,Q.D., Zhang,W., Robinson,M.D., Mnaimneh,S., Chang,R., Pan,Q., Sat,E. *et al.* (2005) Genome-wide analysis of mouse transcripts using exon microarrays and factor graphs. *Nat. Genet.*, **37**, 991–996.
25. Drobyshev,A.L., Machka,C., Horsch,M., Seltmann,M., Liebscher,V., Hrabe de Angelis,M. and Beckers,J. (2003) Specificity assessment from fractionation experiments (SAFE): a novel method to evaluate microarray probe specificity based on hybridisation stringencies. *Nucleic Acids Res.*, **31**, E1–1.
26. Lausted,C., Dahl,T., Warren,C., King,K., Smith,K., Johnson,M., Saleem,R., Aitchison,J., Hood,L. *et al.* (2004) POSaM: a fast, flexible, open-source, inkjet oligonucleotide synthesizer and microarrayer. *Genome Biol.*, **5**, R58.
27. Hughes,T.R., Mao,M., Jones,A.R., Burchard,J., Marton,M.J., Shannon,K.W., Lefkowitz,S.M., Ziman,M., Schelter,J.M. *et al.* (2001) Expression profiling using microarrays fabricated by an inkjet oligonucleotide synthesizer. *Nat. Biotechnol.*, **19**, 342–347.
28. Epstein,J.R., Leung,A.P., Lee,K.H. and Walt,D.R. (2003) High-density, microsphere-based fiber optic DNA microarrays. *Biosens. Bioelectron*, **18**, 541–546.
29. Pozhitkov,A., Chernov,B., Yershov,G. and Noble,P.A. (2005) Evaluation of gel-pad oligonucleotide microarray technology by using artificial neural networks. *Appl. Environ. Microbiol.*, **71**, 8663–8676.
30. Liu,W.T., Wu,J.H., Li,E.S. and Selamat,E.S. (2005) Emission characteristics of fluorescent labels with respect to temperature changes and subsequent effects on DNA microchip studies. *Appl. Environ. Microbiol.*, **71**, 6453–6457.
31. Pozhitkov,A.E., Stedtfeld,R.D., Hashsham,S.A. and Noble,P.A. (2007) Revision of the nonequilibrium thermal dissociation and stringent washing approaches for identification of mixed nucleic acid targets by microarrays. *Nucleic Acids Res*, **35**, e70.
32. Markham,N.R. and Zuker,M. (2005) DINAMelt web server for nucleic acid melting prediction. *Nucleic Acids Res.*, **33**, W577–581.
33. SantaLucia,J. Jr, Allawi,H.T. and Seneviratne,P.A. (1996) Improved nearest-neighbor parameters for predicting DNA duplex stability. *Biochemistry*, **35**, 3555–3562.
34. Xu,J. and Craig,S.L. (2005) Thermodynamics of DNA hybridization on gold nanoparticles. *J. Am. Chem. Soc.*, **127**, 13227–13231.
35. Fotin,A.V., Drobyshev,A.L., Proudnikov,D.Y., Perov,A.N. and Mirzabekov,A.D. (1998) Parallel thermodynamic analysis of duplexes on oligodeoxyribonucleotide microchips. *Nucleic Acids Res.*, **26**, 1515–1521.
36. Vainrub,A. and Pettitt,B.M. (2002) Coulomb blockage of hybridization in two-dimensional DNA arrays. *Phys. Rev. E. Stat. Nonlin. Soft Matter Phys.*, **66**, 041905.
37. Luebke,K.J., Balog,R.P. and Garner,H.R. (2003) Prioritized selection of oligodeoxyribonucleotide probes for efficient hybridization to RNA transcripts. *Nucleic Acids Res.*, **31**, 750–758.
38. Bruun,G.M., Wernersson,R., Juncker,A.S., Willenbrock,H. and Nielsen,H.B. (2007) Improving comparability between microarray probe signals by thermodynamic intensity correction. *Nucleic Acids Res*, **35**, e48.